Magnetic-field control of the electric polarization in $BiMnO_3$

I. V. Solovyev[1,*] and Z. V. Pchelkina[2]
[1]*National Institute for Materials Science, 1-2-1 Sengen, Tsukuba, Ibaraki 305-0047, Japan*
[2]*Institute of Metal Physics, Ural Division, Russian Academy of Sciences, 620041 Ekaterinburg GSP-170, Russia*
(Received 11 July 2010; revised manuscript received 23 August 2010; published 15 September 2010)

We present the microscopic theory of improper multiferroicity in $BiMnO_3$, which can be summarized as follows: (1) the ferroelectric polarization is driven by the hidden antiferromagnetic order in the otherwise centrosymmetric $C2/c$ structure; (2) the relativistic spin-orbit interaction is responsible for the canted spin ferromagnetism. Our analysis is supported by numerical calculations of electronic polarization using the Berry-phase formalism, which was applied to the low-energy model of $BiMnO_3$ derived from the first-principles calculations. We explicitly show how the electric polarization can be controlled by the magnetic field and argue that $BiMnO_3$ is a rare and potentially interesting material where ferroelectricity can indeed coexist and interplay with the ferromagnetism.

DOI: 10.1103/PhysRevB.82.094425 PACS number(s): 75.85.+t, 75.25.Dk, 75.47.Lx

I. INTRODUCTION

Today, the term "multiferroics" is typically understood in a broad sense, as the systems exhibiting spontaneous electric polarization and any type of magnetic ordering.[1] Such materials have a great potential for practical applications in magnetic memories, logic, and magnetoelectric sensors, and therefore attracted enormous attention recently. Beside practical motivation, there is a strong fundamental interest in unveiling the microscopic mechanism of coupling between electric polarization and magnetic degrees of freedom. Nevertheless, the combination of ferroelectricity and *ferro*magnetism, what the term "multiferroicity" was originally introduced for, is rare. Such a combination would, for example, provide an easy way for manipulating the electric polarization **P** by the external magnetic field, which is coupled linearly to the net ferromagnetic moment, etc. The canonical example of the system, where spontaneous electric polarization was believed to coexist with the ferromagnetic ground state, is $BiMnO_3$. However, the origin of such coexistence is largely unknown. Originally, the ferroelectric activity in $BiMnO_3$ was attributed to the highly distorted perovskite structure stabilized by the Bi $6s$ "lone pairs."[2] However, more resent experimental studies (Ref. 3) and first-principles calculations (Ref. 4) suggested that the atomic displacements alone result in the centrosymmetric $C2/c$ structure, which is incompatible with any ferroelectricity. In our previous papers (Refs. 5 and 6), we put forward the idea that the ferroelectric activity in $BiMnO_3$ could be improper and associated with some hidden antiferromagnetic order, which breaks the inversion symmetry. The purpose of this work is to provide the complete quantitative explanation for the appearance and behavior of the ferroelectric polarization in $BiMnO_3$ based on the Berry-phase formalism.[7–9]

II. METHOD

The basic idea of our approach is to construct an effective Hubbard-type model,

$$\hat{\mathcal{H}} = \sum_{ij}\sum_{\alpha\beta} t_{ij}^{\alpha\beta}\hat{c}_{i\alpha}^{\dagger}\hat{c}_{j\beta} + \frac{1}{2}\sum_{i}\sum_{\alpha\beta\gamma\delta} U_{\alpha\beta\gamma\delta}\hat{c}_{i\alpha}^{\dagger}\hat{c}_{i\gamma}^{\dagger}\hat{c}_{i\beta}\hat{c}_{i\delta} \quad (1)$$

for the Mn $3d$ bands near the Fermi level and to include the effect of all other (inactive) states to the definition of the model parameters of the Hamiltonian $\hat{\mathcal{H}}$. Thus, the model is constructed in the basis of 40 Wannier functions in each unit cell (including three t_{2g} and two e_g orbitals for each spin and for each of the four Mn sites), by starting from the electronic structure in the local-density approximation (LDA). The Greek symbols in Eq. (1) denote the combination of spin and orbital indices. All parameters of the model Hamiltonian (1) are defined rigorously, on the basis of the density-functional theory (DFT). The details can be found in the review article (Ref. 10) and in our previous publications (Refs. 5 and 6). Briefly, the one-electron part ($t_{ij}^{\alpha\beta}$) is derived by using a generalized downfolding method. One of the most important parameters in $t_{ij}^{\alpha\beta}$ is the large (about 1.5 eV) crystal-field splitting between two e_g levels, which is caused by the Jahn-Teller distortion and manifests itself in the orbital ordering. The screened Coulomb interactions ($U_{\alpha\beta\gamma\delta}$) are derived by combining the constrained DFT technique with the random-phase approximation (RPA),[10] namely, the screening by outer electrons (such as the $4sp$ electrons of transition metals) and the change in the spatial extension of the atomic wave functions upon the change in their occupation numbers can be easily taken into account by solving the Kohn-Sham equations within constrained DFT approach. On the other hand, the "self-screening" by the same type of electrons, which contribute to other bands due to the hybridization effects (for example, the $3d$ electrons in the oxygen band will strongly screen the Coulomb interactions in the $3d$ band near the Fermi level), can be treated in the perturbative RPA scheme. The self-screening is a very important channel of screening in solids, which substantially reduces the value of the effective Coulomb repulsion U (defined as the screened Slater integral F^0) in the $3d$ band of manganites.[11] In $BiMnO_3$, it is only about 2.3 eV,[5] that has important consequences on the behavior of interatomic magnetic interactions.

The model (1) is solved in the Hartree-Fock approximation,[10]

$$(\hat{t}_{\mathbf{k}} + \hat{\mathcal{V}})|C_{n\mathbf{k}}\rangle = \varepsilon_{n\mathbf{k}}|C_{n\mathbf{k}}\rangle,$$

where $\hat{t}_{\mathbf{k}}$ is the Fourier image of $\hat{t}_{ij}=\|t_{ij}^{\alpha\beta}\|$ and, if necessary, includes the relativistic spin-orbit interaction (SOI), $\hat{\mathcal{V}}$ is the self-consistent Hartree-Fock method, and $|C_{n\mathbf{k}}\rangle$ is the eigenvector in the basis of Wannier functions (where the spin indices are included in the definition of n).

Once the orbital degeneracy is lifted by the strong lattice distortion, the Hartree-Fock theory provides a good approximation for the ground-state properties. The effect of correlation interactions, which can be treated as a perturbation to the Hartree-Fock solution,[10] on the magnetic ground state of manganites is partially compensated by the magnetic polarization of the oxygen states: if the former tend to stabilize antiferromagnetic structures, the latter favors the ferromagnetic alignment.[11] Due to this compensation, the mean-field Hartree-Fock theory, formulated for the minimal $3d$ model, appears to be rather successful for the analysis of the ground-state properties of manganites.

III. MAGNETISM AND THE INVERSION SYMMETRY BREAKING

First, let us explain the main idea of our previous work.[5,6] What is the possible origin of multiferroic behavior of $BiMnO_3$ and how can it be controlled by the magnetic field?

(1) The lattice distortion leads the orbital ordering, which is schematically shown in Fig. 1 in two pseudocubic planes (the orbital ordering in the $y'z'$ plane is similar to the one in the $z'x'$ plane).

This orbital ordering predetermines the behavior of interatomic magnetic interactions, which obey some general principles, applicable for manganites with both monoclinic ($C2/c$) and orthorhombic ($Pbnm$) structure,[5,11] namely, besides conventional nearest-neighbor interactions (shown by hatched lines), one can expect some longer-range interactions between remote Mn atoms, which operate via intermediate Mn sites. These sites are shown by arrows.

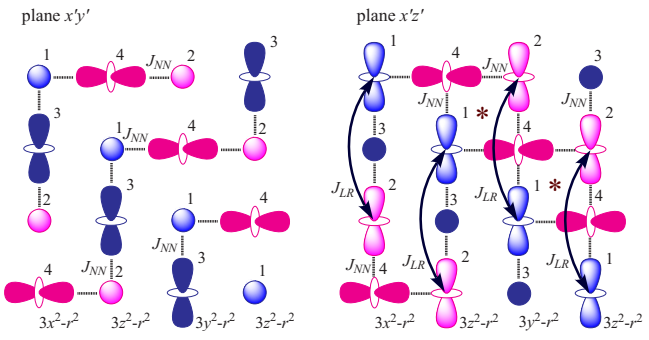

FIG. 1. (Color online) Schematic view on the orbital ordering and corresponding interatomic magnetic interactions in the pseudocubic $x'y'$ and $z'x'$ planes. In the unit cell of $BiMnO_3$, there are four Mn sites (indicated by numbers), which form two inequivalent subgroups: (1,2) and (3,4). The nearest-neighbor ferromagnetic interactions J_{NN} operate in the hatched bonds. The atoms involved in the longer range antiferromagnetic interactions J_{LR} are denoted by arrows. The inversion centers are marked by $*$.

(2) Why should the longer-range interactions exist? The answer is directly related to the fact that the on-site Coulomb repulsion U is not particularly large. Therefore, besides conventional superexchange processes, there are other interactions, which formally appear in the higher orders of the $1/U$ expansion and connect more remote sites. This mechanism is rather similar to the superexchange interaction via intermediate oxygen sites, except that the role of the oxygen states here is played by the unoccupied e_g orbitals of the intermediate Mn sites.[11] By mapping the Hartree-Fock total energies onto the Heisenberg model, one can obtain the following parameters of interatomic magnetic interactions:[5,12] $J_{NN}\sim 5$ and 6 meV (where two slightly different values correspond to inequivalent bonds) and $J_{LR}\sim -3$ meV. Thus, these interactions are at least comparable. Besides them, there are finite (of the order -1 meV) interactions in the bonds 1–2 and 4–4 across the inversion center, which define the final type of the magnetic ground state of $BiMnO_3$.

(3) Without spin-orbit coupling, the longer-range interactions tend to stabilize the antiferromagnetic $\uparrow\downarrow\downarrow\uparrow$ structure (where the arrows denote the directions of spins for the four Mn sites in the unit cell). This antiferromagnetic order destroys the inversion centers (shown by "$*$" in Fig. 1) and thus could be the cause of the ferroelectric activity. Since the $\uparrow\downarrow\downarrow\uparrow$ antiferromagnetic structure satisfies the symmetry operation $\hat{T}\otimes\{m_y|\mathbf{R}_3/2\}$ (where m_y is the mirror reflection $y\rightarrow -y$ associated with the one half of the monoclinic translation $\mathbf{R}_3$, and $\hat{T}$ in the nonrelativistic case flips the directions of spins, which are not affected by m_y), $\mathbf{P}$ is expected to lie in the zx plane.[13] There is an important difference between monoclinic $BiMnO_3$ and orthorhombic systems, such as $HoMnO_3$.[14] In the latter case, the positions of the Mn sites coincide with the inversion centers. Therefore, in order to break the inversion symmetry by a magnetic order, the latter should double (triple, etc.) the orthorhombic unit cell. In $BiMnO_3$, however, the inversion centers are located in interstitial positions and can be destroyed already by an antiferromagnetic arrangement of spins within the same unit cell. Thus, we would like to emphasize again that the origin of the ferroelectric polarization in $BiMnO_3$ is essentially nonrelativistic. It is not related to a noncollinear spin texture either: the collinear antiferromagnetic arrangement of spins is sufficient to break the inversion symmetry and thus produce a finite electric polarization.

(4) Thus, the ferroelectric activity in $BiMnO_3$ could be caused by the antiferromagnetic order. However, this conclusion seems to contradict to another experimental fact, according to which $BiMnO_3$ is a good ferromagnet.[3] This contradiction can be reconciled by considering the relativistic spin-orbit interaction, which is responsible for the weak ferromagnetism. Since the SOI-induced ferromagnetic magnetization is additionally stabilized by isotropic interactions J_{NN}, the ferromagnetism is not so "weak," and the magnetic structure, obtained in the Hartree-Fock calculations for the low-energy model, is strongly noncollinear (Fig. 2). It belongs to the space group Cc, where the only nontrivial symmetry operation is $\{m_y|\mathbf{R}_3/2\}$ and the magnetic moments in the relativistic case are transformed by m_y as auxiliary vectors. Thus, the net ferromagnetic moment is aligned along the y axis,

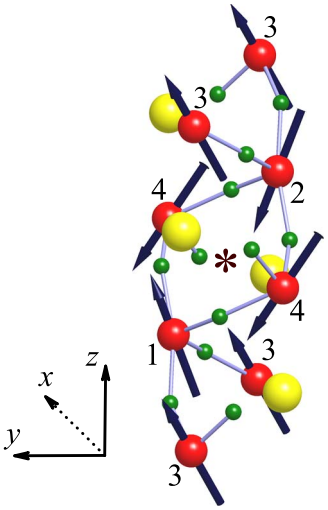

FIG. 2. (Color online) Fragment of the crystal and magnetic structure corresponding to the lowest Hartree-Fock energy. The Bi atoms are indicated by the big light gray (yellow) spheres, the Mn atoms are indicated by the medium gray (red) spheres, and the oxygen atoms are indicated by the small gray (green) spheres. The directions of spin magnetic moments are shown by arrows. The inversion center is marked by the symbol $*$. The left lower part of the figure explains the orientation of the Cartesian coordinate frame. The numerical values of the magnetic moments $\mathbf{M}=(M_x,M_y,M_z)$, measures in μ_B in the Cartesian coordinate frame, are $\mathbf{M}^{1,2}=(\mp 0.08, 1.45, \pm 3.69)$ and $\mathbf{M}^{3,4}=(\pm 0.97, 2.02, \pm 3.27)$.[6]

while the x and z components form the antiferromagnetic structure. Other magnetic configurations have higher energies. The details can be found in Ref. 6 but here we would like to emphasize again that the role of the spin-orbit interaction is to produce the ferromagnetic component of the spin magnetization via the spin canting. It is *not* the source of the ferroelectric polarization in $BiMnO_3$.

By summarizing this part, the $C2/c$ symmetry in $BiMnO_3$ is spontaneously broken by the hidden antiferromagnetic order. The true magnetic ground state of $BiMnO_3$ is strongly noncollinear, where the ferromagnetic order along the y axis coexists with the antiferromagnetic order, and related to it ferroelectric polarization, along the x and z axes. Our scenario not only explains the rare coexistence of ferroelectricity and ferromagnetism but also shows how the electric polarization $\mathbf{P}$ (and the symmetry of $BiMnO_3$) can be controlled by the external magnetic field $\mathbf{B}=(0,B_y,0)$ coupled to the ferromagnetic magnetization. This idea was formulated in Ref. 6. In the present work, we will further consolidate this picture by estimating the numerical values of $\mathbf{P}$ and discussing details of its behavior in the external magnetic field.

IV. ELECTRONIC POLARIZATION

Since the crystal structure of $BiMnO_3$ has the inversion symmetry, there will be no ionic contribution to $\mathbf{P}$, and the main mechanism, which will be considered below, is of purely electronic origin. In principle, the magnetoelastic interactions in the $\uparrow\downarrow\downarrow\uparrow$ structure may cause the atomic displacements away from the centrosymmetric positions and give rise to the ionic term. Nevertheless, such calculations would require the full structural optimization, which cannot be easily incorporated in the model analysis. The first-principles calculations for $HoMnO_3$ show that electronic and ionic terms are at least comparable.[14] Therefore, we expect that the electronic contribution alone could provide a good semiquantitative estimate for $\mathbf{P}$. Moreover, the behavior of electronic polarization presents a fundamental interest as it allows one to explain how $\mathbf{P}$ in improper multiferroics is induced solely by the magnetic symmetry breaking.

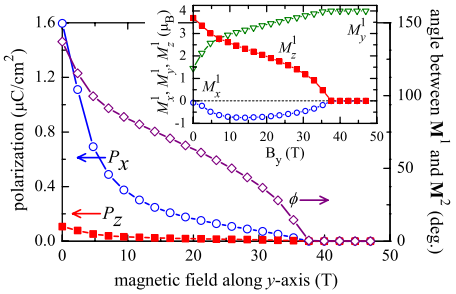

FIG. 3. (Color online) Magnetic-field dependence of the electric polarization, the angle ϕ between spin magnetic moments at the Mn sites 1 and 2, and three components of the vector of the magnetic moment at the site 1 in the Cartesian coordinate frame (shown in the inset).

The modern theory of electric polarization allows one to relate the change in $\mathbf{P}$ to Berry's phase of Bloch electrons.[7–9] It is particularly convenient to use the formulation proposed by Resta, where Berry's phase is computed on the discrete grid of $\mathbf{k}$ points, generated by the $N_1\times N_2\times N_3$ divisions of the reciprocal-lattice vectors $\{\mathbf{G}_a\}$.[9] Then, the position of each point in the Brillouin zone is specified by the three integer indices $(0\le s_a<N_a)$,

$$\mathbf{k}_{s_1,s_2,s_3}=\frac{s_1}{N_1}\mathbf{G}_1+\frac{s_2}{N_2}\mathbf{G}_2+\frac{s_3}{N_3}\mathbf{G}_3,$$

and three components of the electric polarization in the curvilinear coordinate frame, formed by $\mathbf{G}_1$, $\mathbf{G}_2$, and $\mathbf{G}_3$, can be found as[9]

$$\Delta P_a=-\frac{1}{V}\frac{N_a}{N_1N_2N_3}[\gamma_a(\infty)-\gamma_a(0)], \tag{2}$$

where V is the unit-cell volume,

$$\gamma_1=-\sum_{s_2=0}^{N_2-1}\sum_{s_3=0}^{N_3-1}\mathrm{Im}\ln\prod_{s_1=0}^{N_1-1}\det S(\mathbf{k}_{s_1,s_2,s_3},\mathbf{k}_{s_1+1,s_2,s_3}), \tag{3}$$

and similar expressions hold for γ_2 and γ_3. Equation (2) implies that the only meaningful quantity in the bulk is the polarization difference between two states that can be connected by an adiabatic switching process.[7–9]

In the present case, $S=\|\langle C_{n\mathbf{k}}|C_{n'\mathbf{k}'}\rangle\|$ is the overlap matrix, constructed from the Hartree-Fock eigenvectors $|C_{n\mathbf{k}}\rangle$ in the occupied part of the spectrum, taken in two neighboring $\mathbf{k}$ points: $\mathbf{k}=\mathbf{k}_{s_1,s_2,s_3}$ and $\mathbf{k}'=\mathbf{k}_{s_1+1,s_2,s_3}$ for γ_1, etc.[15] The polarization [Eq. (2)] was first computed in the curvilinear coor-

dinate frame and then transformed to the Cartesian frame shown in Fig. 2.[13] In all the calculations, we used the mesh of $72\times72\times36$ points in the Brillouin zone.

As will become clear below, one possible example of the adiabatic switching process, which can be used in the calculations of **P**, is to restore the inversion symmetry by placing the system in the high magnetic field and then adiabatically switching off the field. In practical calculations, however, one can typically use some particular choice of phase in $|C_{n\mathbf{k}}\rangle$ and enforce the equality $\gamma_a=0$ for the centrosymmetric systems.[15] In this context, the discrete Eq. (3) appears to be especially useful because it cancels out the contributions of accidental phases in $|C_{n\mathbf{k}}\rangle$, which can emerge in the process of numerical diagonalization of Hartree-Fock equations in different **k** points.[9] Moreover, it enforces the periodicity of the Hartree-Fock eigenvectors in the reciprocal space: $|C_{n\mathbf{k}}\rangle = |C_{n\mathbf{k}+\mathbf{G}_a}\rangle$, which corresponds to some particular choice of phase.[7]

First, let us discuss results without spin-orbit interaction. As pointed out in the previous section, the antiferromagnetic alignment of spins at the sites 1 and 2 breaks the inversion symmetry and yields finite electric polarization. However, the symmetry of the system also depends on the magnetic configuration in the sublattice 3–4. The electric polarization for the $\uparrow\downarrow\downarrow\uparrow$ structure lies in the zx plane ($P_x=2.1\ \mu\mathrm{C/cm^2}$ and $P_z=0.1\ \mu\mathrm{C/cm^2}$), in agreement with the symmetry arguments presented in Ref. 6. The $\uparrow\downarrow\downarrow\uparrow$ structure can be transformed to the $\uparrow\downarrow\uparrow\downarrow$ one with the same energy by the symmetry operation $\{C_y^2|\mathbf{R}_3/2\}$ (where C_y^2 is the 180° rotation around the y axis), which changes the direction of **P**: $P_{x(z)}\rightarrow -P_{x(z)}$. On the other hand, the $\uparrow\downarrow\downarrow\downarrow$ structure (which has higher energy) is transformed to itself by $\{C_y^2|\mathbf{R}_3/2\}$, and corresponding electric polarization is parallel to the y axis ($P_y=4.8\ \mu\mathrm{C/cm^2}$). Other magnetic structures, characterized by the ferromagnetic alignment of spins at the sites 1 and 2 (such as $\uparrow\uparrow\uparrow\uparrow$, $\uparrow\uparrow\uparrow\downarrow$, and $\uparrow\uparrow\downarrow\downarrow$), preserve the inversion symmetry and result in zero net polarization.

Furthermore, without spin-orbit interaction one can easily evaluate separate contributions to **P** of the states with different projections of spins ($\uparrow$ and $\downarrow$). For the $\uparrow\downarrow\downarrow\uparrow$ structure, the vector of the electric polarization takes the following form: $\mathbf{P}^{\uparrow,\downarrow}=\frac{1}{2}(P_x,\pm P_y,P_z)$, where $P_y=5.7\ \mu\mathrm{C/cm^2}$, and the values of P_x and P_y are listed above. This result is very natural, because the distribution of the electron density for each spin does not have any symmetry and, therefore, the electric polarization $\mathbf{P}^{\uparrow,\downarrow}$ has all three components. On the other hand, the electron density with the spin $\uparrow$ in the $\uparrow\downarrow\downarrow\uparrow$ antiferromagnetic structure can be transformed to the one with the spin $\downarrow$ by the symmetry operation $\{m_y|\mathbf{R}_3/2\}$ and, therefore, $P_y^{\uparrow}=-P_y^{\downarrow}$. Thus, in the total polarization $\mathbf{P}=\mathbf{P}^{\uparrow}+\mathbf{P}^{\downarrow}$, the x and z components with different spins will sum up, while the largest y components will cancel each other.

One can also evaluate the individual contributions to **P** coming from the t_{2g} and e_g bands, which is separated by an energy gap.[5] This yields $P_x^{t_{2g}}=-0.8\ \mu\mathrm{C/cm^2}$, $P_z^{t_{2g}}=-0.3\ \mu\mathrm{C/cm^2}$, $P_x^{e_g}=2.9\ \mu\mathrm{C/cm^2}$, and $P_z^{e_g}=0.4\ \mu\mathrm{C/cm^2}$. Thus, the t_{2g} band is polarized *opposite* to the e_g band, that substantially reduces the value of **P**. Similar tendency was found in the first-principles calculations for orthorhombic manganites.[16]

The spin-orbit interaction results in the canting of spins away from the collinear $\uparrow\downarrow\downarrow\uparrow$ antiferromagnetic state and toward the ferromagnetic alignment. It will *reduce* the value of **P**. In the Hartree-Fock ground state (see Fig. 2), the angle ϕ between spin magnetic moments at the sites 1 and 2 is reduced from 180° till 137°, and corresponding electric polarization parallel to the x axis is reduced from $P_x=2.1\ \mu\mathrm{C/cm^2}$ till $1.6\ \mu\mathrm{C/cm^2}$ while the small component of **P** parallel to the z axis practically does not change ($P_z=0.1\ \mu\mathrm{C/cm^2}$). This effect can be further controlled by the magnetic field, which is applied along the y axis and saturates the ferromagnetic magnetization. Since the absolute value of the local magnetic moment is nearly conserved, the increase in the ferromagnetic component along the y axis will be compensated by the decrease in two antiferromagnetic components along the x and z axes. The corresponding ferroelectric polarization will also decrease. Results of Hartree-Fock calculations in the magnetic field are shown in Fig. 3.[17] Sufficiently large magnetic field (~35 T) will align the magnetic moments at the sites 1 and 2 ferromagnetically ($\phi=0$) and restore the $C2/c$ symmetry.[6] The electric polarization follows the change in ϕ and completely disappears when $\phi=0$. However, the decline of **P** is much steeper, for example, P_x and P_z are reduced by factor two already in the moderate field $B_y\sim5$ T, corresponding to $\phi\sim100°$. Moreover, P_z is always substantially smaller than P_x.

V. CONCLUDING REMARKS

We have proposed the microscopic theory of improper multiferroicity in $BiMnO_3$, which is based on the inversion symmetry breaking by the hidden antiferromagnetic order. We have estimated the ferroelectric polarization and explicitly shown how it can be controlled by the magnetic field. Our scenario still needs to be checked experimentally, and apparently one important question here is how to separate the intrinsic ferroelectricity in $BiMnO_3$ from extrinsic effects, caused by the defects. For example, the values of the ferroelectric polarization obtained in the present work, although comparable with those calculated for other improper ferroelectrics on the basis of manganites,[14] are substantially larger than the experimental value $0.062\ \mu\mathrm{C/cm^2}$ (at 87 K), which was reported so far for $BiMnO_3$.[18] Nevertheless, we believe that systematic study of manganites with the monoclinic $C2/c$ symmetry and finding conditions, which would lead to the practical realization of scenario proposed in our work, presents a very important direction, because it gives a possibility for combining and intermanipulating the *ferroelectricity* and *ferromagnetism* within one sample.

ACKNOWLEDGMENTS

This work is partly supported by Grant-in-Aid for Scientific Research (C) No. 20540337 from MEXT, Japan and Russian Federal Agency for Science and Innovations, Grant No. 02.740.11.0217.

*solovyev.igor@nims.go.jp

[1] D. Khomskii, Physics **2**, 20 (2009).
[2] R. Seshadri and N. A. Hill, Chem. Mater. **13**, 2892 (2001).
[3] A. A. Belik, S. Iikubo, T. Yokosawa, K. Kodama, M. Igawa, S. Shamoto, M. Azuma, M. Takano, K. Kimoto, Y. Matsui, and E. Takayama-Muromachi, J. Am. Chem. Soc. **129**, 971 (2007).
[4] P. Baettig, R. Seshadri, and N. A. Spaldin, J. Am. Chem. Soc. **129**, 9854 (2007).
[5] I. V. Solovyev and Z. V. Pchelkina, New J. Phys. **10**, 073021 (2008).
[6] I. V. Solovyev and Z. V. Pchelkina, Pis'ma Zh. Eksp. Teor. Fiz. **89**, 701 (2009) [JETP Lett. **89**, 597 (2009)].
[7] D. Vanderbilt and R. D. King-Smith, Phys. Rev. B **48**, 4442 (1993).
[8] R. Resta, Rev. Mod. Phys. **66**, 899 (1994).
[9] R. Resta, J. Phys.: Condens. Matter **22**, 123201 (2010).
[10] I. V. Solovyev, J. Phys.: Condens. Matter **20**, 293201 (2008).
[11] I. Solovyev, J. Phys. Soc. Jpn. **78**, 054710 (2009).
[12] The interatomic magnetic interactions are defined as one half of the Hartree-Fock energy difference between antiferromagnetic and ferromagnetic configurations in each bond.
[13] We use the following setting for the monoclinic translations: $\mathbf{R}_{1,2}=\frac{1}{2}(\sin\beta a, \mp b, \cos\beta a)$ and $\mathbf{R}_3=(0,0,c)$. The positions of four Mn atoms in the unit cell are specified by the vectors: $\boldsymbol{\tau}_1 = y_{\mathrm{Mn}}(\mathbf{R}_1-\mathbf{R}_2)+\frac{1}{4}\mathbf{R}_3$, $\boldsymbol{\tau}_2=-\boldsymbol{\tau}_1$, $\boldsymbol{\tau}_3=\frac{1}{2}\mathbf{R}_1$, and $\boldsymbol{\tau}_4=\frac{1}{2}(\mathbf{R}_2+\mathbf{R}_3)$. The experimental structure parameters were taken from Ref. 3. More detailed information about the settings, which were used for the crystal structure of $BiMnO_3$, can be found in Refs. 5 and 6.
[14] S. Picozzi, K. Yamauchi, B. Sanyal, I. A. Sergienko, and E. Dagotto, Phys. Rev. Lett. **99**, 227201 (2007).
[15] Some caution should be taken when choosing the phases of the Bloch functions. In order to minimize the effect of the basis (Wannier) functions $W^{\boldsymbol{\tau}}_{\mathbf{R}}(\mathbf{r})$, centered at the site $\boldsymbol{\tau}$ of the unit cell $\mathbf{R}$, the Bloch functions were defined as $W^{\boldsymbol{\tau}}_{\mathbf{k}}(\mathbf{r})=\frac{1}{\sqrt{N}}\Sigma_{\mathbf{R}}e^{i\mathbf{k}\cdot(\boldsymbol{\tau}+\mathbf{R})}W^{\boldsymbol{\tau}}_{\mathbf{R}}(\mathbf{r})$. Then, the matrix elements $\langle W^{\boldsymbol{\tau}}_{\mathbf{R}}|\mathbf{r}-\mathbf{R}-\boldsymbol{\tau}|W^{\boldsymbol{\tau}}_{\mathbf{R}}\rangle$ of $\mathbf{P}$ in the basis of $\{W^{\boldsymbol{\tau}}_{\mathbf{R}}\}$ will either vanish or cancel each other since the low-energy model and, therefore, $\{W^{\boldsymbol{\tau}}_{\mathbf{R}}\}$ themselves are defined by starting from the nonmagnetic LDA band structure (Ref. 10), which preserves the inversion symmetry. Thus, the main contribution to $\mathbf{P}$ in our model analysis arises from the evolution of $|C_{n\mathbf{k}}\rangle$.
[16] K. Yamauchi, F. Freimuth, S. Blügel, and S. Picozzi, Phys. Rev. B **78**, 014403 (2008).
[17] The interaction term with the magnetic field is given by $\hat{\mathcal{H}}_B=-\mu_B\mathbf{B}\cdot(2\hat{\mathbf{s}}+\hat{\mathbf{l}})$, where $\hat{\mathbf{s}}$ and $\hat{\mathbf{l}}$ are the operators of spin and orbital angular momentum, respectively.
[18] A. Moreira dos Santos, A. K. Cheetham, T. Atou, Y. Syono, Y. Yamaguchi, K. Ohoyama, H. Chiba, and C. N. R. Rao, Solid State Commun. **122**, 49 (2002).